FEBS Letters

FEBS PRESS science publishing by scientists

Giardia lamblia Hsp90 pre-mRNAs undergo self-splicing to generate mature RNA in an *in vitro* trans-splicing reaction

Vinithra Iyer, Sivarajan T. Chettiar, Manish Grover, Purusharth Rajyaguru, Rishi Kumar Nageshan and Utpal Tatu

Department of Biochemistry, Indian Institute of Science, Bangalore, India

Correspondence
U. Tatu, Department of Biochemistry, Indian Institute of Science, Bangalore – 560012, India
Tel: +91 (080) 22932823
E-mail: tatu@iisc.ac.in, tatu@biochem.iisc.ernet.in

(Received 23 November 2018, accepted 26 December 2018, available online 22 January 2019)

doi:10.1002/1873-3468.13324

Edited by Claus Azzalin

We have previously shown that the Heat Shock Protein 90 (Hsp90) gene in *G. lamblia* is expressed from two ORFs localized 777 kb apart. The pre-mRNAs transcribed from these ORFs are stitched by a trans-splicing mechanism. Here, we provide mechanistic details of this process by reconstituting the reaction using *in vitro* synthesized pre-mRNA substrates. Using RT-PCR, northern blot and nanostring technology, we demonstrate that the *in vitro* synthesized pre-mRNAs have the capability to self-splice in the absence of nuclear proteins. Inhibition of the trans-splicing reaction using a ssDNA oligo corresponding to a 26-nucleotide complementary sequence confirmed their role in juxtapositioning the pre-mRNA substrates during the self-splicing reaction. Our study provides the first example of a self catalysed, trans-splicing reaction in eukaryotes.

Keywords: *G. lamblia*; heat shock protein 90; molecular chaperone; post-transcriptional regulation; RNA repair; RNA splicing

Giardia lamblia is an early branching human and animal parasite that infects over a billion people worldwide [1,2]. *Giardia* genome is intron poor with only six genes containing cis-spliced introns [3–7].

Previous studies from our lab have shown that hsp90 gene in *G. lamblia* is encoded by two different ORFs separated by a 777-kb-long intervening sequence on chromosome 5. These ORFs are designated as *hspN* (GL50803_98054) and *hspC* (GL50803_13864), containing the N-terminal and C-terminal regions of the protein respectively [8]. However, the mechanism by which these ORFs generate full-length mRNA are not fully understood.

As the first step towards understanding the mechanism of this RNA repair event, we reconstituted *Hsp90* trans-splicing reaction *in vitro*, using purified *in vitro* transcribed *hspN* and *hspC* pre-mRNAs. Our study for the first time shows that the pre-mRNAs of Hsp90 get trans-spliced *in vitro* in the absence of spliceosomal proteins and snRNAs by a self-splicing reaction. In addition to emphasizing the role of Mg^{2+} ions, our study also highlights the importance of 26-nucleotide complementary sequences in the pre-mRNAs for the self-splicing reaction.

Materials and methods

In vitro cultivation of *Giardia* Trophozoites

An axenic culture *of G. lamblia* Portland P1 or WB-C6 (assemblage A) parasites were cultured as previously described by Nageshan *et al.* [8,9].

Abbreviations
dhc-β, dynein heavy chain β; *dhc*-ϒ, dynein heavy chain ϒ; *hsp90*, heat shock protein 90; nt(s), nucleotide(s); NTPs, nucleotide triphosphates; SS, splice site; Ts, Trans-splicing; TSP, Trans-spliced product.

Cloning of HspN, HspC and full-length Hsp90 constructs

Using gDNA as template [8] with specific *hspN* and *hspC* primers, a 571-bp region in *hspN* and a 420-bp region in *hspC* ORF was amplified. A 749-bp region (FLHsp90) which contained the trans-spliced (Ts) junction was amplified from the full-length Hsp90 (2.1 kB) previously cloned [10], using *HspN* sense primer and *HspC* antisense primer. These amplicons were ligated to pRSET-C vector under T7 promoter. Detailed information about sequences (in the construct, MCS and primer sequences) is described in Supporting information (Figs S1 and S3).

In vitro transcription

HspN, HspC and FLHsp90 clones were linearized overnight using EcoRI-HF enzyme (Fig. S2). The purified linearized constructs were used for the preparation of pre-mRNAs using T7 RNA polymerase. The integrity of RNAs was checked on 1.2% MOPS-formaldehyde agarose gel (Fig. S3).

Nuclear extract preparation

Giardia nuclear extract was prepared as described by Janet Yee *et al*., with minor modifications [11].

In vitro trans-splicing

Each 100 µl reaction mixture contained 300–500 µg of nuclear protein in 20 mM potassium L-glutamate, 20 mM KCl, 3 mM $MgCl_2$, 20 mM HEPES– KOH, pH 7.7, 20 mM creatine phosphate, 0.48 mg·mL^{-1} creatine kinase, 2.5% poly(ethylene glycol) (M.W-4000), 0.2 mM EDTA, 0.5 mM EGTA, 4 mM DTT,1X PIC (Roche), equal concentrations of pre-mRNA substrates (without 5′m7G cap) and ATP (0.5 mM), and then the trans-splicing reaction was conducted for 15 min at 28 °C.

RT-PCR as an assay to detect *in vitro* trans-splicing

Equal concentration (500 ng) of pre-mRNAs after incubation in the trans-splicing (Ts) buffer were precipitated with isopropanol post phenol–chloroform extraction. Purified RNA was used for the cDNA synthesis with the gene-specific primer (HspC-R). The cDNA was then used as the template for PCR to amplify the trans-spliced junction using specific forward and reverse primers for the Ts junction (Fig. S5).

Preparation of *Giardia* total RNA

Total RNA from *Giardia* trophozoites was prepared using TRI reagent (ambion) using manufacturer's protocol. One hundred nanograms of RNA was used to serve as *in vivo* positive control in the Nanostring platform (Fig. 2B). Two micrograms of total RNA was used for cDNA synthesis (verso cDNA kit) using random hexamers and oligo (dT) primers. The cDNA was subjected to PCR with specific primers as shown in Fig. 1D to serve as *in vivo*-positive control for *in vitro* Ts assay.

Northern blot to visualize *in vitro* trans-spliced product

Eight micrograms of *HspN* and *HspC* pre-mRNAs were incubated in Ts buffer at 28 °C for 15 min. RNA was then

Fig. 1. Hsp90 pre-mRNAs undergo self-splicing *in vitro* in a Mg^{2+}-dependent manner. (A) Schematic representation of *in vitro* trans-splicing assay. The *in vitro* transcribed pre-mRNAs were incubated in the Ts buffer at 28 °C for 15 min. The RNA was then extracted and subjected to cDNA synthesis using gene-specific primer and the trans-spliced product was detected by PCR with primers complementary to *hspN* and *hspC* pre-mRNAs. (B) *Hsp90* pre-mRNAs of *G. lamblia* undergo self-splicing *in vitro*. RT-PCR and PCR as the *in vitro* trans-splicing assay with primers for trans-spliced product confirms the self-splicing ability of the pre-mRNAs. Lanes 1–4 involved use of primers, one annealing to *hspN* and the other annealing to *hspC*, to amplify the junction from cDNA. Lane 1 and 3 confirms the presence of faint and fuzzy trans-spliced amplicon in the presence of nuclear extract and ATP and presence of nuclear extract only; Lanes 2 and 4 show the presence of trans-spliced amplicon in the absence of nuclear extract alone and nuclear extract and ATP. Lane 8 shows the trans-spliced amplicon from the FLRNA which serves as the positive control. (C) Sanger's DNA sequencing confirms the self-splicing ability of the pre-mRNAs. Sequencing result obtained with forward primer (RO2-F) and reverse primer (RO2-R) confirms the presence of trans-spliced junctional sequence in the mature *in vitro* self-spliced product (from Fig. 1B, lane 4). Sequence highlighted with box completely matches with the sequencing result and the Ts junction is demarcated. Nucleotides underlined represent the sites where forward and reverse primers hybridize on the cDNA template. (D) *In vitro* Ts assay with additional primers for the Ts junction confirms the self-splicing ability of the pre-mRNA substrates. Lanes 3, 4 and 5 show the Ts amplicon of expected sizes with HspN-F, C-R primers, RO1 and RO2 primers respectively. Lanes 1 and 2 serve as internal control for Ts assay indicating the presence of pre-mRNA substrates in the assay tube. Lanes 6–10 serve as *in vivo*-positive control. (E) Direct visualization of self-spliced RNA by northern blot. α^{32}P-dATP body labelled DNA probe containing the Ts junctional sequence hybridizes with the self-spliced product in lane 1 and FLRNA in lane 4 which served as the positive control. Lanes 2 and 3 where the HspN and HspC pre-mRNA substrates were incubated alone in the Ts buffer does not display the self-spliced band and served as the negative control. (F) *In vitro* self-splicing reaction requires presence of Mg^{2+} ions. Lane 1 shows a self-spliced amplicon in the presence of Mg^{2+} ions. Self-spliced amplicon is absent in the absence of Mg^{2+}ions (lane 3), in the presence of EDTA (lane 2) and in the presence of EDTA alone (Lane 4). Lane 8 contains the trans-spliced amplicon from the FLRNA which served as the positive control.

denatured and resolved on 2% MOPS-formaldehyde agarose gel and transferred to nylon membrane overnight. RNA was UV cross-linked to the membrane and hybridized overnight in hybridization buffer with a 400 bp α^{32}P-dATP body-labelled DNA probe which had the Ts junction sequence. The membrane was then subjected to

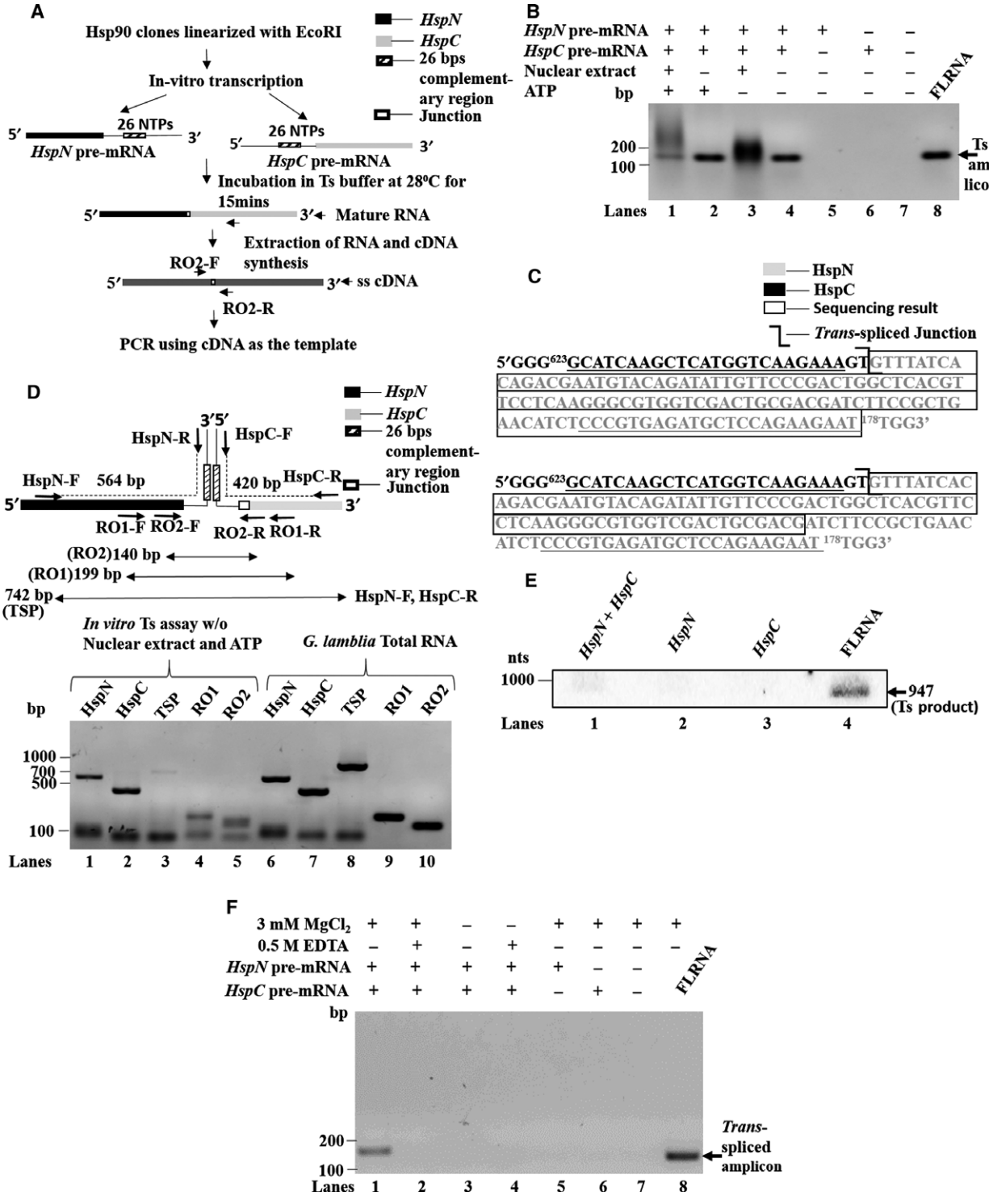

stringency washes and RNA bands on the membrane were then visualized by autoradiography.

Nanostring technology

A pair of probes, reporter (Probe A) and capture probes (Probe B), was designed for each target RNA species (Table S1 and Fig. S8). One hundred nanograms of RNA from each Ts assay tube after quality control (Table S2 and Fig. S9) was subjected to hybridization separately with a cocktail of excess reporter and capture probes designed to detect all target RNA under this study. Hybridization was conducted overnight at 67 °C. The tripartite complexes were then purified from unbound and excess probes. The different barcodes corresponding to different target RNA species were visualized and counted using fluorescence microscope, each count corresponding to one copy of the transcript [12].

Inverse PCR for generating HspN and HspC deletion mutants

5′ phosphorylated forward and reverse primers were designed pointing outwards to exclude the 26 bp region in both the clones. The linear mutant bands after PCR were subjected to ligation and transformed in *E. coli* DH5α competent cells. Colonies harbouring the mutant plasmids were selected by colony PCR and confirmed by sequencing.

Oligo inhibition assay

Increasing amounts of Anti-N26 DNA oligo were incubated along with a definite number of molecules of HspN pre-mRNA in the Ts buffer at 65 °C for 5 min and snap chilled on ice for 2 min. Equimolar amounts of HspC pre-mRNA were then introduced in the Ts buffer and incubated at 28 °C for 15 min. RNA was purified from DNA oligos and equal concentration of RNA from each assay tube was subjected to cDNA synthesis. The cDNA was then subjected to Q-PCR using primers which would amplify the Ts junction. Q-PCR quantitation results were reported as Mean with SD. For paired comparisons, one-tailed paired t-test was used. All analysis was done using GraphPad Prism 5.

Results

HspN and HspC pre-mRNAs self-splice *in vitro*

To reconstitute the trans-splicing reaction *in vitro*, pre-mRNA substrates were prepared by *in vitro* transcription reaction using plasmids containing *hspN* and *hspC* fragments. The fragments from hspN and hspC ORFs contain all the essential elements for the splicing reaction, including 26 nucleotide positioning elements, 5′ and 3′ splice sites and the branch point adenine.

HspN and HspC pre-mRNAs were synthesized and used for the reconstitution assay as described in materials and methods. Full-length (FL) Hsp90 RNA (FLRNA), 947 nucleotides long, was similarly generated and used as positive control. The integrity of the *in vitro* transcribed hspN, hspC pre-mRNAs and the FL Hsp90 RNA (FLRNA) were examined on 1.2% MOPs-Formaldehyde Agarose Gel (Fig. S3).

We prepared nuclear extract from actively dividing *Giardia* trophozoites culture as described in the materials and methods. We incubated equal concentrations of pre-mRNA substrates with or without nuclear extract from *G. lamblia* for 15 min at 28 °C in trans-splicing (Ts) buffer. At the end of the reaction, we extracted RNA and prepared cDNA using a gene-specific primer. The cDNA was then subjected to PCR amplifications by using primers for the trans-spliced product (TSP). The full-length *in vitro* trans-spliced RNA was expected to give an amplicon of 140 bp. Hsp90 full-length mRNA (FLRNA), which was treated in parallel was used as the positive control.

As shown in Fig. 1B, when the two pre-mRNA substrates were incubated in the presence of nuclear extract and ATP, an amplicon of expected size was found (Fig. 1B, lane 1), a similar sized band was seen in full-length control suggesting that the 140 bp amplicon corresponded to the trans-spliced product. The band was completely absent in the buffer alone, or having only one of the two RNA substrates (Lane 5–7). A fuzzy band of correct size was obtained on inclusion of nuclear extract but absence of ATP (Fig. 1B, lane 3).

Importantly, we found a specific 140 bp product corresponding to trans-spliced RNA when we used RNA substrates without the presence of nuclear extract, both in the presence and the absence of exogenously added ATP (Fig. 1B, lane 2 and 4), suggesting the self-splicing ability of the pre-mRNAs. To further confirm that the 140 bp reaction product indeed corresponded to trans-spliced product, the amplicon was gel eluted and sequence was confirmed by DNA sequencing as shown in Figs. 1C and S6.

In addition to primers which amplify 140 bp trans-spliced junction (RO2-F,R), we used two additional pairs of primers (RO1-F,R and HspN-F, HspC-R), in each pair the forward primer binds to HspN sequence and the reverse primer to HspC sequence, as shown in the schematic (Fig. 1D). Ts amplicon of expected sizes were obtained with all three pairs of primers confirming the self-splicing ability of the pre-mRNAs. Lanes 1 and 2 (Fig. 1D) serve as internal control indicating the

presence of pre-mRNA substrates, HspN and HspC in the reaction tube when amplified using HspN and HspC sequence-specific primers. *Giardia* total RNA was subjected to cDNA synthesis and PCR with specific primers (Fig. 1D, lanes 6–10) to serve as the *in vivo* positive control.

Our results suggested that the two pre-mRNA substrates contain all the structural features sufficient to facilitate the trans-splicing reaction resulting in the formation of mature product formed between GU-AG splice sites and containing the expected junction sequence [8].

To directly visualize self-splicing ability of the two pre-mRNAs, we performed northern blotting to detect the self-spliced band as described in Materials and methods. As shown in Fig. 1E, lane 1, the α^{32}P-dATP body-labelled DNA probe, containing the Ts junction sequence, could detect the presence of self-spliced product at the expected size of 947 nucleotides. The DNA probe did not detect the Ts product when the pre-mRNA substrates were incubated alone in the Ts buffer (lanes 2 and 3). FLRNA (lane 4) harbouring the Ts junctional sequence served as the positive control. Thus, the northern blot provides direct evidence for the self-splicing capability of pre-mRNAs.

Self-splicing is Mg^{2+} dependent

Mg^{2+} ions are known to be involved in the stabilization of the oxyanion leaving group at the 5′ splice site of the exon 1 of group I and group II self-splicing reactions. Mg^{2+} ions are also established to stabilize the transition state of the first trans-esterification reaction [13,14]. It appears that similar to the canonical cis-splicing reaction, Mg^{2+} ions may be required in the first trans-esterfication step of *Hsp90 in vitro* self-splicing (Fig. 1F). To investigate the importance of metal ions in the trans-splicing buffer for the molecular stitching event *in vitro,* the Ts reaction was conducted in the presence of Mg^{2+} ions and 0.5M EDTA in different combinations in the Ts buffer at 28 °C for 15 min. The RNA was extracted, cDNA prepared and the product was identified by PCR. The self-spliced product was detected in the presence of Mg^{2+} (Lane 1) but was not detected in the absence of Mg^{2+} (Lane 3). The self-spliced product was absent when the reaction was conducted in the presence of both 0.5 M EDTA and Mg^{2+} ions (Lanes 2); or in the presence of 0.5M EDTA alone (Lane 4). However, occasionally, the size of the self-spliced amplicon was observed to be higher by 33 nucleotides (173 bps) than the FLRNA-positive control. The higher molecular weight band obtained in lane 1 was because of an additional 33 nucleotides that were contributed from the intronic region of hspC pre-mRNA in addition to the trans-spliced (Ts) junctional sequence confirmed by Sanger's DNA sequencing (Fig. S7). The FLRNA containing the Ts junction was used as the positive control which showed a PCR product of 140 bps (Lane 8). The result suggested that *in vitro* self-splicing reaction is Mg^{2+} ion dependent and the occasional presence of a 173 bp product could be attributed to low fidelity of the *in vitro* self-splicing reaction in the absence of any nuclear protein interactors.

Nanostring platform validates the presence of trans-spliced junction in the self-spliced product

Nanostring technology allows multiplexed direct and precise detection of RNA transcripts. This technology requires no enzymatic or amplification steps thus making it an unbiased platform to detect unique RNA species. Nanostring platform relies on a simple hybridization chemistry of specific reporter and capture probes designed to be complementary to the target RNA species.

We designed two probes, reporter (probe A, with unique fluorescent barcode) and capture probe (probe B, with biotin moiety) for each of the four RNA targets, purified pre-mRNA substrates HspN and HspC and products, trans-spliced mature Hsp90 mRNA and the branched lariat by-product generated after *in vitro* trans-splicing assay. (Fig. S8).

In vitro trans-splicing assay was performed as above. A cocktail of all reporter and capture probes for all targets under this study was hybridized at 67 °C overnight with 100 ng of extracted RNA from each assay tube, separately. Simplified schematic for nanostring assay procedure is described in Fig. 2A [12].

As shown in Fig. 2B, the nanostring platform could detect precisely the number of molecules of mature self-spliced mRNAs (79 940) and the branched lariat by-product (19 419) in 100 ng of RNA extracted after the trans-splicing reaction. Assay tubes containing HspN and HspC pre-mRNAs alone showed the presence of only the corresponding pre-mRNAs. FLRNA incubated under similar conditions in the Ts buffer showed the presence of the trans-spliced junction and served as the positive control for the assay. Total RNA extracted from *Giardia* trophozoites served as the *in vivo*-positive control with most of the pre-mRNA substrates consumed to give rise to mature mRNA.

Thus, the nanostring platform validated and confirmed the presence of *in vitro*-generated trans-spliced

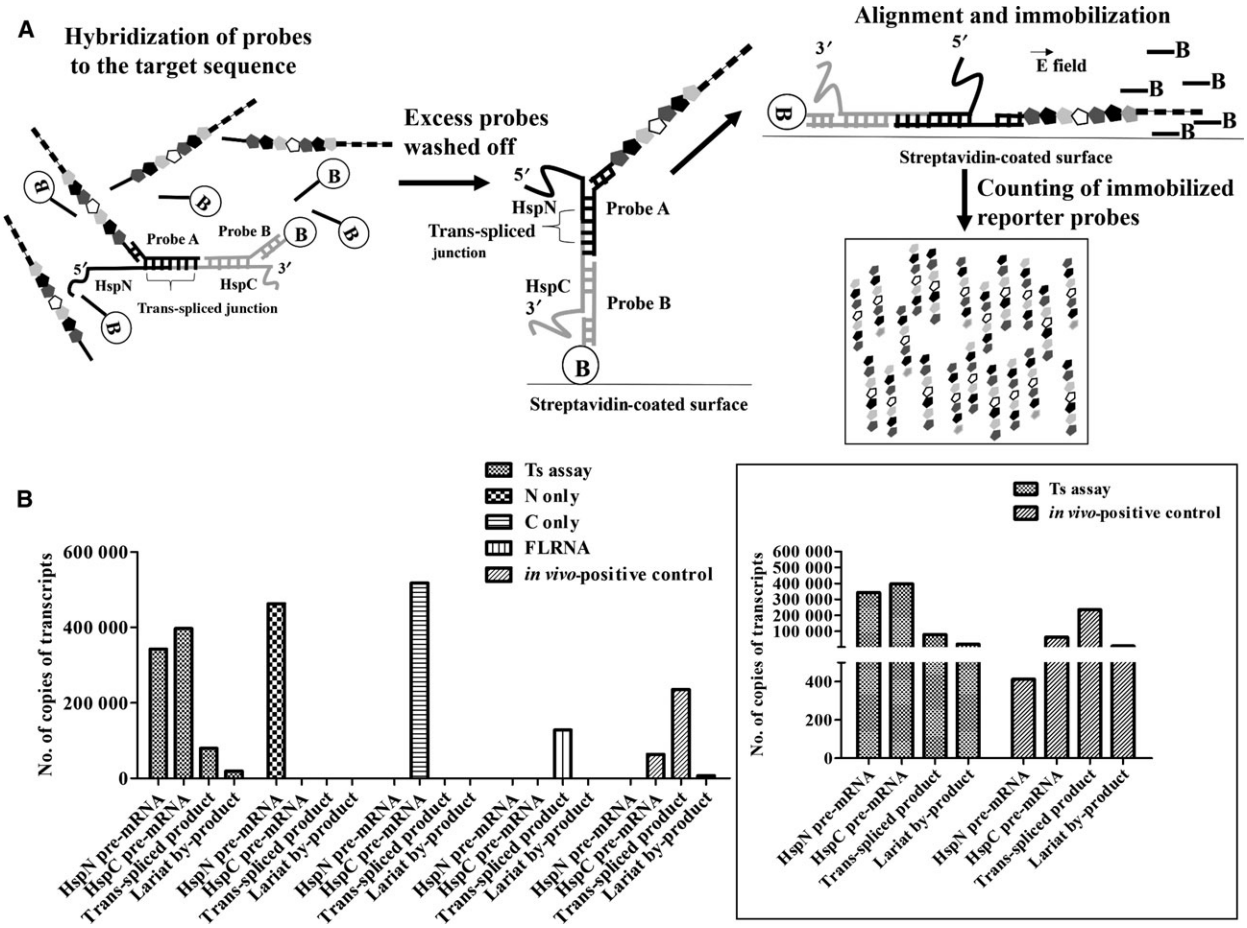

Fig. 2. Nanostring platform confirms the self-splicing ability of Hsp90 pre-mRNAs. (A) Schematic representation of the workflow of nanostring platform. RNA extracted from assay tubes after incubation in the Ts buffer were subjected to hybridization overnight at 67 °C, with reporter and capture probe cocktail. Post hybridization, the tripartite complexes in each tube were washed to remove the unbound probes during its transit through microfluidic cartridge. The Probe–target complexes were then aligned under the influence of electric field and immobilized on streptavidin coated surface with the help of biotinylated oligos complementary to the repetitive DNA sequences present towards the 3′ end of the reporter probe. Aligned molecular barcodes were then visualized and counted using a fluorescence microscope and a CCD camera. (B) Nanostring platform confirms the presence of *in vitro* generated trans-spliced junction in the absence of spliceosomal proteins. Nanostring technology detects 79 940 copies of trans-spliced mature RNA and 19 419 copies of branched lariat by-product upon incubation of equal concentrations of purified pre-mRNA substrates HspN and HspC in the Ts buffer lacking spliceosomal proteins. RNA extracted from assay tubes containing HspN and HspC alone shows the presence of only the corresponding pre-mRNAs which served as the negative control. FLRNA harbouring the trans-spliced junction when incubated alone under similar conditions in the Ts buffer shows counts corresponding to only the junctional sequence and hence served as the positive control for our assay. *Giardia* total RNA served as the *in vivo* positive control with most of the pre-mRNA substrates consumed to give rise to the mature RNA. Figure in the inset was plotted with an expanded *Y*-axis to have an expanded view of copies of Ts reaction products.

mature Hsp90 mRNA and the lariat by-product *in vitro*.

26 nucleotide positioning elements in the pre-mRNAs are necessary for self-splicing reaction

All the trans-spliced genes, *hsp90*, *dhc*-β and *dhc-Y* identified in *Giardia* harbour complementary sequence elements in the corresponding split genes [4,8,15]. This appears to be a strategy to bring together individual pre-mRNAs to facilitate their joining. To test the importance of the 26-nucleotide sequence elements in Hsp90 self-splicing reaction, we generated mutant plasmids lacking just the 26 nucleotide positioning elements by inverse PCR approach as described in Materials and methods. The modified plasmids were used as template for *in vitro* transcription and RNA

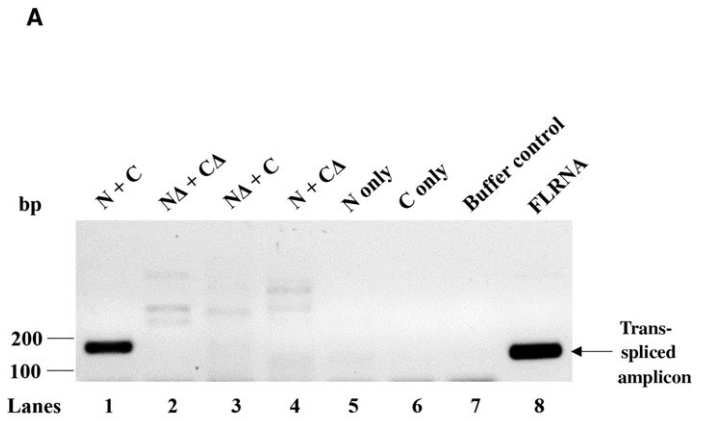

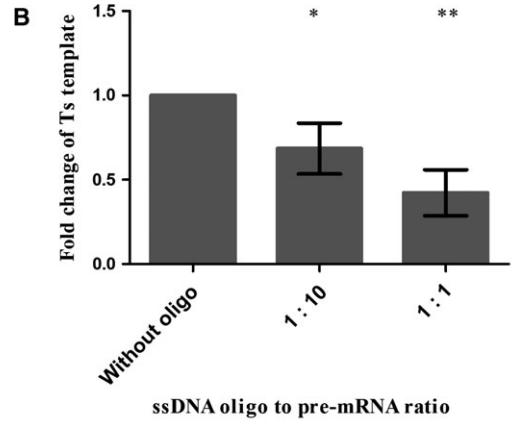

C_t (Threshold cycle)	With-out oligo	1 : 10	1 : 1
1.	31.38	31.60	32.24
2.	29.19	29.90	30.38
3.	31.48	32.25	33.32

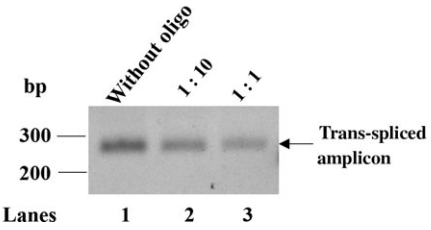

Fig. 3. 26-nucleotide complementary sequences in Hsp90 pre-mRNAs are essential for self-splicing reaction. (A) Lane 1 shows a single, intense self-spliced band at the expected size, when *hspN* and *C* pre-mRNAs were incubated in the Ts buffer. Lane 2, shows multiple PCR products with primers specific for the junction, upon using the mutated pre-mRNAs. Lanes 3 and 4 shows smear like pattern when different combinations of mutated and unmodified pre-mRNAs were used in the splicing assay. Lanes 5–7 serve as the negative control with no amplification observed in buffer only and when either of the two pre-mRNAs were present. Lane 8 contains the trans-spliced amplicon from the FLRNA which served as the positive control. (B) ssDNA oligo inhibition assay confirms that the 26-nucleotide complementary sequences in the pre-mRNAs are essential for *in vitro* self-splicing reaction. Anti-N26 ssDNA oligo was allowed to hybridize with *HspN* pre-mRNA prior to incubation with equimolar amounts of *HspC* pre-mRNA. Presence of oligo in the ratio of 1:10 with the pre-mRNAs decreased the self-spliced template by 20% as compared to control, ($P = 0.0342$, $n = 3$) as shown in the upper panel quantitated using Q-PCR. The Ts template decreased by 60% ($P = 0.091$, $n = 3$) as compared to control when ssDNA oligo was introduced in the ratio of 1:1 with the pre-mRNAs. Lower panel shows the reaction products resolved on 1.4% agarose gel post Q-PCR, to confirm the size of the Ts product. Lanes 1, 2 and 3 shows a 293 bp Ts product with a decreasing intensity of the product with a concomitant increase in ssDNA oligo.

purified as above. The mutant pre-mRNAs were incubated in the Ts buffer at 28 °C for 15 min. The RNA was extracted, cDNA prepared and the product was identified by PCR. As shown in Fig. 3A, lane 1, pre-mRNAs containing the 26 nucleotide complementary sequences yielded an intense self-spliced band of the expected size. Lane 2 (Fig. 3A) shows a smear with primers specific for trans-spliced junction. Also, the expected trans-spliced amplicon was absent when the mutant and unmodified pre-mRNA were used in different combinations (Lanes 3 and 4). The band was completely absent in the buffer alone, or having only one of the two RNA substrates without the mutation (Lane 5–7). FLRNA treated in parallel under similar conditions yielded an intense band of 140 bp and served as the positive control for the *in vitro* Ts assay. The faint, multiple bands observed in lanes 2, 3 and 4 could be due to the inability of the pre-mRNAs to choose the correct corresponding 5′ and 3′ splice sites resulting in promiscuous pairing of exons.

We used DNA oligo inhibition assay to confirm the importance of 26-nucleotide complementary sequences in hsp90 *in vitro* self-splicing reaction. We incubated increasing amounts of ssDNA oligo complementary to the 26 nucleotides in the *hspN* pre-mRNA (Anti-N26 DNA oligo) with *hspN* pre-mRNA in the Ts buffer for 5 min at 65 °C followed by snap chilling on ice for 2 min. *HspC* pre-mRNA was then introduced into the reaction buffer at an equimolar concentration and incubated at 28 °C for 15 min. RNA was purified from the DNA oligo and equal concentrations of RNA from each tube was subjected to cDNA synthesis and real time PCR analysis as described in Materials and methods.

As shown in Fig. 3B (lanes 1, 2 and 3), Q-PCR gave rise to a 293 bp product containing the Ts junction. When anti-N26 oligo and pre-mRNAs were incubated in the ratio of 1:10, the self-spliced product decreased by 20% as compared to the control reaction without DNA oligo (Fig. 3B). In equimolar concentration of DNA oligo, the self-spliced product decreased by 60% as compared to the control in the absence of the DNA oligo. To confirm the size of the amplified products in the presence of increasing oligo, the Q-PCR products were resolved on 1.4% agarose gel. Lanes 1, 2 and 3 show the self-spliced band (293 bp) with a decrease in intensity with a concomitant increase in ssDNA oligo.

Our results confirmed that the 26-nucleotide positioning elements in the pre-mRNA substrates, by virtue of its complementary base pairing interactions may guide proper orientation of the 5′ splice site and branch point adenine for the first nucleophillic attack at the 5′ splice site and subsequently the choice of the correct 3′ splice site in the second nucleophillic attack.

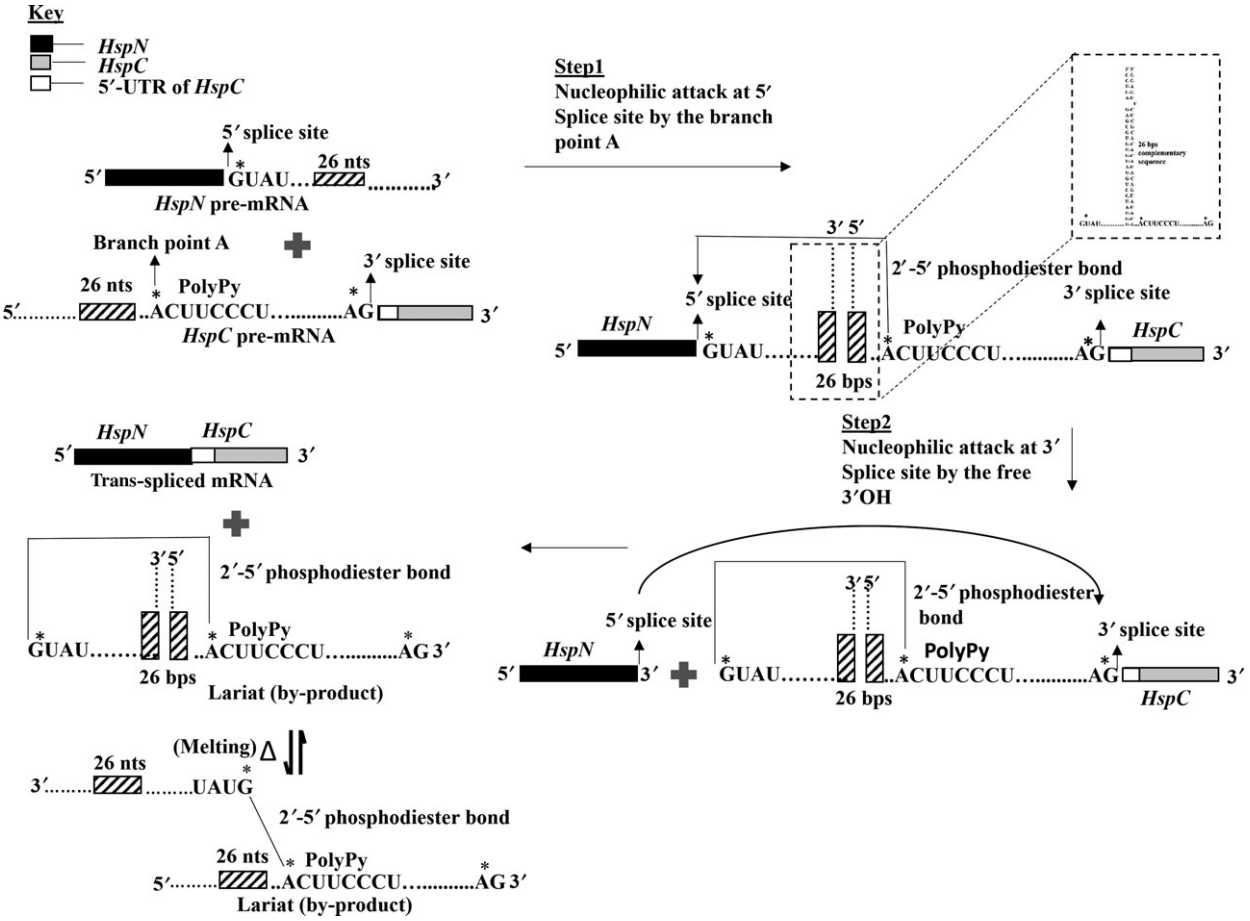

Fig. 4. Mechanism of trans-splicing reaction. The first step of the trans-splicing reaction is facilitated by the intermolecular interaction between 26-nucleotide positioning elements in *hspN* and *hspC* pre-mRNAs orienting the residues, branch point adenine and 5′SS, participating in the first nucleophillic attack. This orientation step may be the most critical step for the trans-splicing reaction which may be aided by spliceosomal protein components *in vivo*. After the first nucleophilic attack, the second attack at the 3′splice site forms the trans-spliced product and generates an unstable lariat by-product.

Mechanism of the *in vitro* trans-splicing reaction

Our data suggest a model wherein complementary base pairing between the 26-nucleotide positioning elements of the two pre-mRNAs bring the catalytic branch point adenine of *hspC* pre-mRNA in proximity of the 5′SS of *hspN* pre-mRNA to initiate the first nucleophillic attack. This step would generate a free 3′OH in the *hspN* pre-mRNA which nucleophillically attacks the 3′ splice site generating the full-length Hsp90 mature mRNA and the lariat by-product (Fig. 4). Our results suggest that all the information necessary for the Ts reaction is present within the pre-mRNA sequences and the spliceosomal components may facilitate the Ts reaction to ensure fidelity and efficiency of the reaction *in vivo*.

Discussion

Cis-splicing in eukaryotes proceeds via two transesterification reactions. In the first step, the 2′OH of a canonical branch point adenine preceding the polypyrimidine tract attacks the 5′ splice site (upstream of canonical GU residues) to form a free 3′OH at the 5′ exon boundary. The free 3′OH attacks the 3′ splice site of the next exon (downstream of AG residues), thus releasing the lariat and the cis-spliced product. This is essentially an intramolecular reaction [16–18]. Trans-splicing on the other hand, is an intermolecular reaction [19].

Our study shows that the pre-mRNAs of Hsp90 can get trans-spliced *in vitro* in the absence of spliceosomal proteins in Mg^{2+}dependent manner. Self-splicing ability of pre-mRNA substrates was confirmed by an RT-PCR approach and directly without any amplification steps by northern blot. We also confirmed this unique splicing reaction using a simple hybridization chemistry employing specific fluorescently tagged and biotinylated probes to detect the self-spliced product and the highly unstable lariat by-product.

Unlike the well-studied intramolecular cis-splicing mechanism, the trans-splicing reaction described here is an intermolecular reaction between independently transcribed RNA from ORFs located at distant locations in the *G. lamblia* genome [8]. The presence of 26-nucleotide positioning elements in the introns appears to overcome this spatial displacement and facilitate the RNA precursors to interact and thereby support the trans-splicing reaction.

Our study provides first experimental evidence for the role of 26 nucleotide complementary sequences in the two pre-mRNAs. The mutant pre-mRNAs lacking these complementary nucleotides or the presence of an excess of antisense ssDNA oligos to the 26-nucleotide elements robustly inhibits the self-splicing reaction.

Giardia lamblia Hsp90 trans-splicing is reminiscent of the splicing mechanism found in *Caenorhabditis elegans* ERI-6/7 superfamily I helicase where the formation of an intermolecular stem structure brings the two pre-mRNAs together [20]. Two out of three trans-spliced genes discovered so far in *Giardia, hsp90 and dhc-β*, seem to exhibit conservation of all the essential features of a cis-splicing reaction, namely (a) GU-AG boundaries, (b) polypyrimidine tract upstream of the intron-exon junction and (c) an essential adenine for nucleophillic attack.

In vivo however, in addition to these nucleotide elements, involvement of specific RNA-binding proteins may be necessary for the fidelity and efficiency of trans-splicing reaction. In addition, the regulation of spatial organization of hspN and hspC gene in the nucleus to facilitate their physical proximity and thereby the trans-splicing reaction may provide an additional level of regulation for *G. lamblia* Hsp90 gene expression.

Acknowledgements

Authors thank funding for the study by Department of Biotechnology (DBTO-0403) and DBT-IISc Partnership grant. RN and MG acknowledge fellowship from IISc and Council of Scientific and Industrial research (CSIR). We thank Prof. Didier Picard and Prof. Katharina Strub from University of Geneva, Switzerland for their inputs and encouragement during initial stages of this project. Authors thank Department of Parasitology, Post Graduate Institute of Medical Education and Research (PGIMER), Chandigarh, India for providing *Giardia* culture.

Author contributions

VI and SC performed the experiments. RN and MG made the *HspN* and *HspC* constructs. PR gave valuable inputs and suggestions in this work. UT conceived and designed the study and wrote the paper.

References

1 Cacciò SM and Ryan U (2008) Molecular epidemiology of giardiasis. *Mol Biochem Parasitol* **160**, 75–80.
2 Lane S and Lloyd D (2002) Current trends in research into the waterborne parasite *Giardia*. *Crit Rev Microbiol* **28**, 123–147.
3 Nixon JEJ, Wang A, Morrison HG, McArthur AG, Sogin ML, Loftus BJ and Samuelson J (2002) A

spliceosomal intron in *Giardia lamblia*. *Proc Natl Acad Sci USA* **99**, 3701–3705.
4 Roy SW, Hudson AJ, Joseph J, Yee J and Russell AG (2012) Numerous fragmented spliceosomal introns, AT-AC splicing, and an unusual dynein gene expression pathway in *Giardia lamblia*. *Mol Biol Evol* **29**, 43–49.
5 Russell AG, Shutt TE, Watkins RF and Gray MW (2005) An ancient spliceosomal intron in the ribosomal protein L7a gene (Rpl7a) of *Giardia lamblia*. *BMC Evol Biol* **5**, 45.
6 Morrison HG, McArthur AG, Gillin FD, Aley SB, Adam RD, Olsen GJ, Best AA, Cande WZ, Chen F, Cipriano MJ *et al*. (2007) Genomic minimalism in the early diverging intestinal parasite *Giardia lamblia*. *Science* **317**, 1921–1926.
7 Franzén O, Jerlström-Hultqvist J, Einarsson E, Ankarklev J, Ferella M, Andersson B and Svärd SG (2013) Transcriptome profiling of *Giardia* intestinalis using strand-specific RNA-seq. *PLoS Comput Biol* **9**, e1003000.
8 Nageshan RK, Roy N, Hehl AB and Tatu U (2011) Post-transcriptional repair of a split heat shock protein 90 gene by mRNA trans-splicing. *J Biol Chem* **286**, 7116–7122.
9 Diamond LS, Harlow DR and Cunnick CC (1978) A new medium for the axenic cultivation of *Entamoeba histolytica* and other Entamoeba. *Trans R Soc Trop Med Hyg* **72**, 431–432.
10 Nageshan RK, Roy N, Ranade S and Tatu U (2014) Trans-spliced heat shock protein 90 modulates encystation in *Giardia lamblia*. *PLoS Negl Trop Dis* **8**, e2829.
11 Yee J, Mowatt MR, Dennis PP and Nash TE (2000) Transcriptional analysis of the glutamate dehydrogenase gene in the primitive eukaryote, *Giardia lamblia*. Identification of a primordial gene promoter. *J Biol Chem* **275**, 11432–11439.
12 Geiss GK, Bumgarner RE, Birditt B, Dahl T, Dowidar N, Dunaway DL, Fell HP, Ferree S, George RD, Grogan T *et al*. (2008) Direct multiplexed measurement of gene expression with color-coded probe pairs. *Nat Biotechnol* **26**, 317–325.
13 Sjögren AS, Pettersson E, Sjöberg BM and Strömberg R (1997) Metal ion interaction with cosubstrate in self-splicing of group I introns. *Nucleic Acids Res* **25**, 648–653.
14 Sontheimer EJ, Gordon PM and Piccirilli JA (1999) Metal ion catalysis during group II intron self-splicing: parallels with the spliceosome. *Genes Dev* **13**, 1729–1741.
15 Kamikawa R, Inagaki Y, Tokoro M, Roger AJ and Hashimoto T (2011) Split introns in the genome of *Giardia* intestinalis are excised by spliceosome-mediated trans-splicing. *Curr Biol CB* **21**, 311–315.
16 Reed R (2000) Mechanisms of fidelity in pre-mRNA splicing. *Curr Opin Cell Biol* **12**, 340–345.
17 Reed R (1996) Initial splice-site recognition and pairing during pre-mRNA splicing. *Curr Opin Genet Dev* **6**, 215–220.
18 Staley JP and Guthrie C (1998) Mechanical devices of the spliceosome: motors, clocks, springs, and things. *Cell* **92**, 315–326.
19 Lei Q, Li C, Zuo Z, Huang C, Cheng H and Zhou R (2016) Evolutionary insights into RNA trans-splicing in vertebrates. *Genome Biol Evol* **8**, 562–577.
20 Fischer SEJ, Butler MD, Pan Q and Ruvkun G (2008) Trans-splicing in *C. elegans* generates the negative RNAi regulator ERI-6/7. *Nature* **455**, 491–496.

Supporting information

Additional supporting information may be found online in the Supporting Information section at the end of the article.

Fig. S1. *Hsp90N* and *Hsp90C* partial sequences; and FLHsp90 sequences cloned in pRSET-C vector.

Fig. S2. Quality check of linearized HspN, HspC and FLHsp90 plasmids on 0.6% agarose gel.

Fig. S3. Integrity of the *in vitro* transcribed *hspN*, *hspC* and FLRNA pre-mRNAs on 1.2% agarose, MOPS-formaldehyde gel.

Fig. S4. PCR amplification of cDNA from *in vitro* trans-splicing reaction with *hspN* and *hspC* primers.

Fig. S5. Schematic representation of the trans-spliced product intermediate along with the hybridization sites of the primers used to detect the self-splicing event *in vitro*.

Fig. S6. Sequence of the self-spliced amplicon.

Fig. S7. Sequence of the higher molecular weight (173 bp) self-spliced amplicon occasionally observed with forward and reverse primers.

Fig. S8. Schematic representation of Reporter (Probe A) and capture probes (Probe B) and their corresponding target sequences in the RNA targets under this study (not to scale).

Fig. S9. Electropherogram profiles.

Table S1. Reporter (Probe A) and capture probe (Probe B) sequences designed to specifically detect the RNA targets under this study.

Table S2. Nanodrop QC details of the RNA samples extracted after *in vitro* Ts reaction and total RNA from log phase culture of *G. lamblia*.